

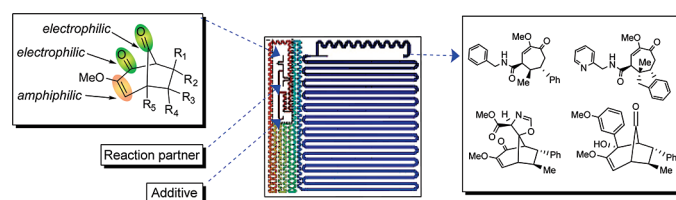
Development of an Automated Microfluidic Reaction Platform for Multidimensional Screening: Reaction Discovery Employing Bicyclo[3.2.1]octanoid Scaffolds

John R. Goodell,[‡] Jonathan P. McMullen,[†] Nikolay Zaborenko,[†] Jason R. Maloney,[‡] Chuan-Xing Ho,[‡] Klavs F. Jensen,^{*,†} John A. Porco Jr.,^{*,†} and Aaron B. Beeler^{*,‡}

[‡]Department of Chemistry and Center for Chemical Methodology and Library Development (CMLD-BU), Boston University, 590 Commonwealth Avenue, Boston, Massachusetts 02215, and [†]Department of Chemical Engineering, Massachusetts Institute of Technology, 77 Massachusetts Avenue, 66-342, Cambridge, Massachusetts 02139.

beelera@bu.edu

Received May 21, 2009



An automated, silicon-based microreactor system has been developed for rapid, low-volume, multidimensional reaction screening. Use of the microfluidic platform to identify transformations of densely functionalized bicyclo[3.2.1]octanoid scaffolds will be described.

Introduction

Historically, major pharmaceutical breakthroughs have been enabled by complex chemical structures—often, complex natural products—with unique biological mechanisms.¹ Recently, there have been numerous efforts to discover new complex chemical scaffolds through organic synthesis.² As part of our interest in the synthesis of new chemotypes and structural frameworks, we recently formulated a new approach to chemical reaction discovery termed “multidimensional reaction screening”.³ In this approach, chemical reactions are evaluated by using multiple variables in an array format. Efforts such as multidimensional reaction screening address an ongoing challenge in drug discovery:

the decreasing availability of new chemical entities for biological screening and the need for discovery of new synthetic methodologies to access novel compounds of interest.⁴

Miniaturization and automation of biological screening have enabled an unprecedented level of throughput.⁵ However, such developments have been slower in the area of chemical reaction discovery.⁶ The recent rise of microfluidic technologies has presented an opportunity for the development of tools to enable small-scale, rapid chemical reactions which may be applied to discovery endeavors.⁷ Herein, we

(1) (a) Balamurugan, R.; Dekker, F. J.; Waldmann, H. *Mol. BioSyst.* **2005**, *1*, 36. (b) Arve, L.; Voigt, T.; Waldmann, H. *QSAR Comb. Sci.* **2006**, *25*, 449.

(2) (a) Schreiber, S. L. *Science* **2000**, *287*, 1964. (b) Tan, D. S. *Nat. Chem. Biol.* **2005**, *1*, 74. (c) Shang, S.; Tan, D. S. *Curr. Opin. Chem. Biol.* **2005**, *9*, 248. (d) Wipf, P.; Coleman, C. M.; Janjic, J. M.; Iyer, P. S.; Fodor, M. D.; Shafer, Y. A.; Stephenson, C. R. J.; Kendall, C.; Day, B. W. *J. Comb. Chem.* **2005**, *7*, 322. (e) Wipf, P.; Werner, S.; Woo, G. H. C.; Stephenson, C. R. J.; Walczak, M. A. A.; Coleman, C. M.; Twining, L. A. *Tetrahedron* **2005**, *61*, 11488. (f) Thomas, G. L.; Wyatt, E. E.; Spring, D. R. *Curr. Opin. Drug Discovery Dev.* **2006**, *9*, 700. (g) Spandl, R. J.; Bender, A.; Spring, D. R. *Org. Biomol. Chem.* **2008**, *6*, 1149.

(3) Beeler, A. B.; Su, S.; Singleton, C. A.; Porco, J. A. Jr. *J. Am. Chem. Soc.* **2007**, *129*, 1413.

(4) For discussion of reaction screening approaches, see: (a) Weber, L.; Illgen, K.; Almstetter, M. *Synlett* **1999**, 366. (b) Kana, W. M.; Rosenman, M. M.; Sakurai, K.; Snyder, T. M.; Liu, D. R. *Nature* **2004**, *431*, 545. (c) Miller, S. J. *Nat. Biotechnol.* **2004**, *22*, 1378.

(5) Liu, B.; Li, S.; Hu, J. *Am. J. Pharmacogenomics* **2004**, *4*, 263.

(6) For examples of automated screening of reaction conditions, see: (a) Harre, M.; Neh, H.; Schulz, C.; Tilstam, U.; Wessa, T.; Weinmann, H. *Org. Process Res. Dev.* **2001**, *5*, 335. (b) von Wangelin, A. J.; Neumann, H.; Gordes, D.; Klaus, S.; Jiao, H.; Spannenberg, A.; Kruger, T.; Wendler, C.; Thurov, K.; Stoll, N.; Beller, M. *Chem.—Eur. J.* **2003**, *9*, 2273. (c) Di, L.; McConnell, O. J.; Kerns, E. H.; Sutherland, A. G. *J. Chromatogr., B* **2004**, *809*, 231. (d) Dinter, C.; Weinmann, H.; Merten, C.; Schutz, A.; Blume, T.; Sander, M.; Harre, M.; Neh, H. *Org. Process Res. Dev.* **2004**, *8*, 482. (e) Rudolph, J.; Lormann, M.; Bolm, C.; Dahmen, S. *Adv. Synth. Catal.* **2005**, *347*, 1361.

(7) For recent reviews on advancements in microfluidics, see: (a) Jensen, K. F. *Chem. Eng. Sci.* **2001**, *56*, 293. (b) Weigl, B. H.; Bardell, R. L.; Cabrera, C. R. *Adv. Drug Delivery Rev.* **2003**, *55*, 349. (c) Pihl, J.; Karlsson, M.; Chiu, D. T. *Drug Discovery Today* **2005**, *10*, 1377.

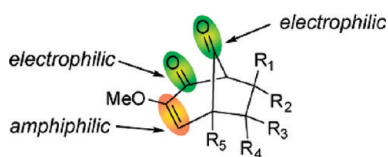


FIGURE 1. Diverse functionality of the bicyclo[3.2.1]octanoid scaffold for multidimensional reaction screening.

report the development of an automated microfluidic platform and a series of multidimensional reaction screens involving bicyclo[3.2.1]octanoid scaffolds,⁸ multifunctional chemotypes⁹ presenting an array of functionality for reaction discovery (Figure 1).

Numerous reports have indicated that reactions performed within microreactors generate products in greater yield and purity and in shorter times in comparison to traditional batch conditions owing to the high heat and mass transfer and capability of obtaining wider ranges of temperature.¹⁰ The continuous flow operations and small volume inherent to microreactors enable multidimensional screening to be performed quickly while minimizing required amounts of reagents. These features also render microreactors as powerful tools for screening applications involving expensive catalysts¹¹ and reagents that are difficult to synthesize in bulk.¹² Additionally, microreactors are ideal for generation of highly reactive intermediates¹³ and for analyzing reaction conditions that cannot be easily achieved with conventional laboratory equipment.¹⁴

Ismagilov and co-workers recently reported studies that highlight the advantages of microfluidic screening as an alternative to the more commonly used 96-well plates.^{15,16} In their study, reactions were preloaded into capillary cartridges as nanoliter plugs (droplets), demonstrating the potential for microfluidic reaction screening. Continuous flow screening conducted by Ley and co-workers¹⁷ represents another approach that offers many of the same advantages of microfluidics. In the current work, we expand the field of reaction screening by introducing an automated microfluidic system capable of selecting chemical reagents and solvents, as well as varying reaction times and temperature.

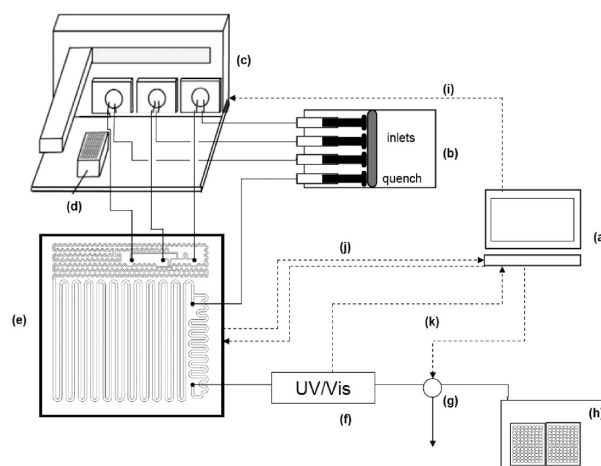


FIGURE 2. Automated microfluidic platform for reaction screening. Components include the following: (a) computer with operating software, (b) multihead syringe pump, (c) liquid handler, (d) 96-well reagent block, (e) compression packaging that houses microreactor and thermoelectric module, (f) UV detection for optical triggering, (g) sampling valve, (h) 96-well plate fraction collector, and feedback control loops (i–k) for reagent injection, temperature control, and sample collection, respectively.

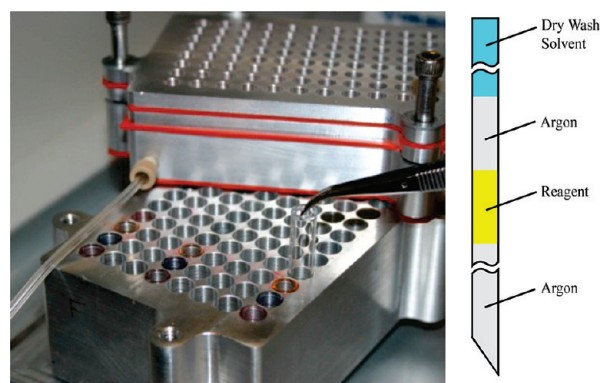


FIGURE 3. Reagent storage block (left) and illustration of inert handling in sample syringes (right).

Results and Discussion

Automated Platform. We have constructed an automated microfluidic platform capable of conducting programmed multidimensional arrays in a sequential format (Figure 2). The ability to perform a series of specified reactions was made possible by the incorporation of a liquid handler equipped with four independently controlled sample probes. To maintain an inert environment for reagents, we designed and fabricated a 96-well reagent block that accommodates commercially available glass sleeves that are sealed with a silicon rubber septum (Figure 3). The integrity of the reagents within the block is maintained by an inert gas chamber mounted over the sample wells. This chamber also serves as a source of inert gas during reagent transfer. During the screening procedure, reagents are drawn from this reagent block by syringes and injected into the microfluidic platform as boluses.

Pulse Flow. Our specific goal was to develop a screening platform capable of executing one to several thousand analytical scale reactions. One microfluidic technique utilizes a two-phase flow system, where the reaction droplets are

- (8) Büchi, G.; Mak, C.-P. *J. Am. Chem. Soc.* **1977**, *99*, 8073.
 (9) For examples of multifunctional scaffolds, see: (a) Couladouros, E. A.; Strongilos, A. T. *Angew. Chem., Int. Ed.* **2002**, *41*, 3677. (b) Kumagai, N.; Muncipinto, G.; Schreiber, S. L. *Angew. Chem., Int. Ed.* **2006**, *45*, 3635. (c) Comer, E.; Rohan, E.; Deng, L.; Porco, J. A. Jr. *Org. Lett.* **2007**, *9*, 2123.
 (10) For recent reviews on microfluidic reactions, see: (a) Fletcher, P. D. I.; Haswell, S. J.; Pombo-Villar, E.; Warrington, B. H.; Watts, P.; Wong, S. Y. F.; Zhang, X. *Tetrahedron* **2002**, *58*, 4735. (b) Hessel, V.; Lowe, H. *Chem. Eng. Technol.* **2005**, *28*, 267. (c) Watts, P.; Haswell, S. J. *Chem. Soc. Rev.* **2005**, *34*, 235. (d) Geyer, K.; Codee, J. D. C.; Seeberger, P. H. *Chem.—Eur. J.* **2006**, *12*, 8434. (e) Watts, P.; Wiles, C. *Chem. Commun.* **2007**, 443.
 (11) Allwardt, A.; Holzmüller-Lau, S.; Wendler, C.; Stoll, N. *Catal. Today* **2008**, *137*, 11.
 (12) Yoshida, J.; Nagaki, A.; Yamada, T. *Chem.—Eur. J.* **2008**, *14*, 7450.
 (13) Usutani, H.; Tomida, Y.; Nagaki, A.; Okamoto, H.; Nokami, T.; Yoshida, J. *J. Am. Chem. Soc.* **2007**, *129*, 3046.
 (14) De Mas, N.; Gunther, A.; Schmidt, M. A.; Jensen, K. F. *Ind. Chem. Eng. Res.* **2003**, *42*, 698.
 (15) Chen, D. L.; Ismagilov, R. F. *Curr. Opin. Chem. Biol.* **2006**, *10*, 226.
 (16) Song, H.; Chen, D. L.; Ismagilov, R. F. *Angew. Chem., Int. Ed.* **2006**, *45*, 7336.
 (17) (a) Baxendale, I. R.; Griffiths-Jones, C. M.; Ley, S. V.; Tranmer, G. K. *Chem.—Eur. J.* **2006**, *12*, 4407. (b) Baxendale, I. R.; Deely, J.; Griffiths-Jones, C. M.; Ley, S. V.; Saaby, S.; Tranmer, G. K. *Chem. Commun.* **2006**, 2566. (c) Baumann, M.; Baxendale, I. R.; Ley, S. V.; Smith, C. D.; Tranmer, G. K. *Org. Lett.* **2006**, *8*, 5231.

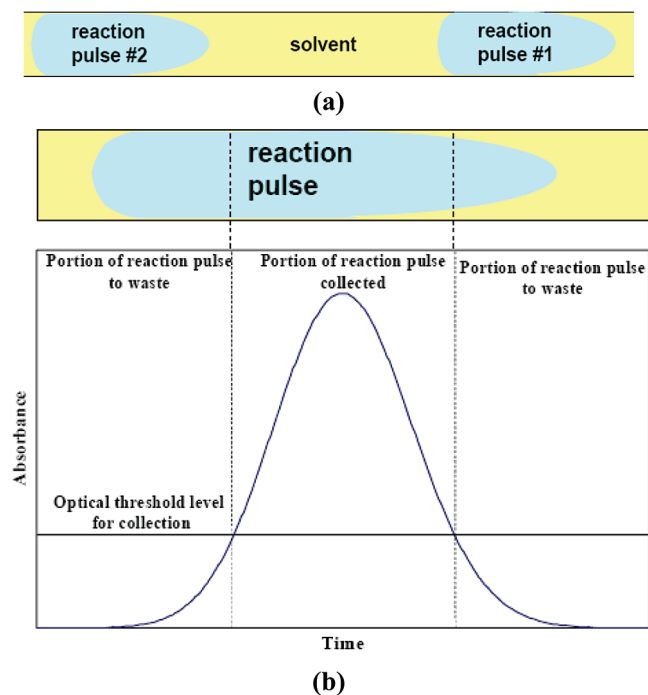


FIGURE 4. (a) Illustration of sequential reaction pulses and the dispersion caused by laminar flow and surface wetting. (b) Example of sample collection via optical triggering. Collection begins and terminates once concentration of reaction pulse crosses a specified threshold, thereby enabling collection of the central portion of the pulse.

separated by a fluorinated carrier fluid or a gas phase.^{15,18,19} However, both of these methods have limitations in reaction screening applications. For example, solubility of the fluorinated liquid into the reaction droplet increases with higher temperatures,²⁰ and the use of a gas phase may lead to cross-contamination of the reaction droplets via the liquid meniscus between two droplets. Therefore, a comprehensive range of reaction conditions without cross-contamination was obtained by injecting reaction pulses into a continuous stream of solvent and by incorporating an optically triggered collection system. As illustrated in Figure 4, reagent pulses (boluses) were individually introduced into the microreactor through the liquid handler and coalesced into a single reaction pulse after entering the microreactor.²¹

A disadvantage of applying this homogeneous flow style is the axial dispersion of the reaction pulses associated with laminar flow (Figure 4a).²² To account for this dispersion, an optically triggered fraction collection system was established to collect the central section of these pulses, while the tail ends were discarded (Figure 4b). The dispersion was also reduced by minimizing dead volumes and the lengths of PTFE tubing between the injector and the reactor. Furthermore, programmed delays between the reaction pulses were incorporated to prevent cross-contamination.

(18) Günther, A.; Jensen, K. F. *Lab Chip* **2006**, *6*, 1487.
 (19) Hatakeyama, T.; Chen, D. L.; Ismagilov, R. F. *J. Am. Chem. Soc.* **2006**, *128*, 2518.
 (20) Gladysz, J. A.; Curran, D. P.; Horvath, I. T. E., *Handbook of Fluorous Chemistry*, 1st. ed.; Wiley-VCH: New York, 2004.
 (21) Garcia-Egido, E.; Spikmans, V.; Wong, S. Y. F.; Warrington, B. H. *Lab Chip* **2003**, *3*, 73.
 (22) Günther, A.; Khan, S. A.; Thalmann, M.; Trachsel, F.; Jensen, K. F. *Lab Chip* **2004**, *4*, 278.

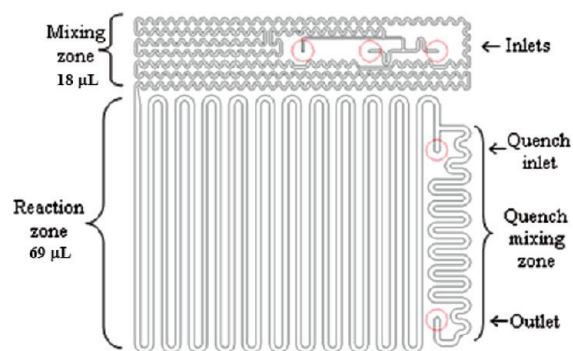


FIGURE 5. Layout of the silicon microreactor used for multidimensional screens.

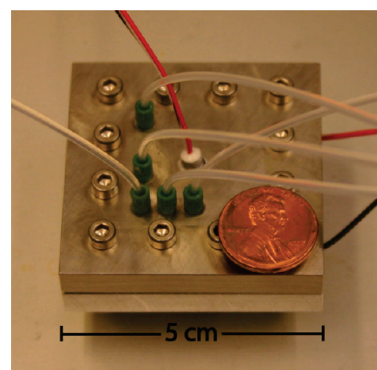


FIGURE 6. Compression packaging unit used in screening applications. The unit houses the microreactor and thermoelectric device used for heating/cooling.

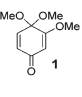
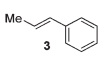
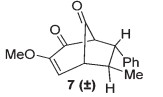
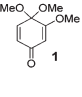
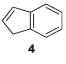
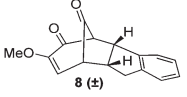
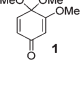
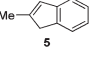
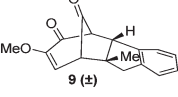
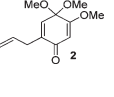
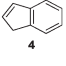
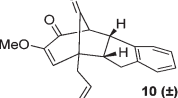
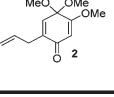
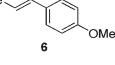
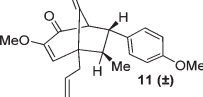
Reactor Design. A silicon microreactor was developed based on a design previously used for liquid-phase²³ and gas-liquid²⁴ reaction optimization. In the current design, use of T-junctions and increased serpentine channels results in improved mixing over a broader range of chemical applications compared to the previous reactor design. The microreactor layout consists of three fluid inlets, followed by an 18 μL mixing zone and a 69 μL reaction zone, which terminate at the quench inlet (Figure 5). The quenched mixture flows through another mixing zone to ensure full and rapid quenching of the reaction.

The microfluidic channels and ports were etched into silicon wafers by a deep reactive ion etch (DRIE). The silicon surface was then oxidized to silica (glass) and anodically bonded to a Pyrex wafer to cap the channels, providing a glass surface that is compatible with most organic solvents. The high thermal conductivity of silicon microreactors results in fast temperature equilibration; its mechanical strength enables reactions to be investigated at pressures up to 100 bar with an appropriate packaging technique.²⁵

Fluidic connections to the chip were achieved with a compression packaging scheme (Figure 6). This compression chuck houses the microreactor and a thermoelectric (TE)

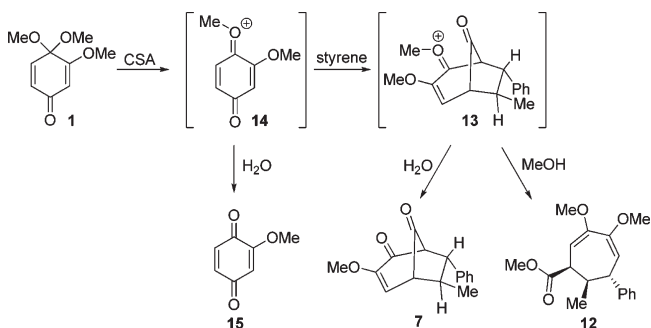
(23) Ratner, D. M.; Murphy, E. R.; Jhunjhunwala, M.; Snyder, D. A.; Jensen, K. F.; Seeberger, P. H. *Chem. Commun.* **2005**, *5*, 578.
 (24) Murphy, E. R.; Martinelli, J. R.; Zaborenko, N.; Buchwald, S. L.; Jensen, K. F. *Angew. Chem., Int. Ed. Engl.* **2007**, *10*, 1734.
 (25) Murphy, E. R.; Inoue, T.; Sahoo, H. R.; Zaborenko, N.; Jensen, K. F. *Lab Chip* **2007**, *7*, 1309.

TABLE 1. Synthesis of Bicyclo[3.2.1]octanoid Substrates^a

entry	monoketal	alkene	product	% yield
1				43 %
2				55 %
3				70 %
4				60 %
5				69 %

^aConditions: alkene (2.0 equiv), dry CSA (1.0 equiv), anhydrous CH₃CN, H₂O (0.75 equiv), rt, 2 h.

SCHEME 1. Synthesis of Bicyclo[3.2.1]octanoid Scaffolds



element capable of heating or cooling the microreactor by adjusting the electric current.^{26,27} The wetted material of the compression piece (top half) is made from stainless steel to ensure compatibility with a broad range of reagents, while the bottom portion is constructed from aluminum to create a sufficient heat sink with high thermal conductivity for the thermoelectric device. The reaction temperature is monitored with a thermoresistor that is in direct contact with the microreactor and is inserted into the top plate.

As previously mentioned, it is necessary for each reagent pulse to enter the main reactor channels simultaneously. Accomplishing this task required the compression piece ports and the inlet channels to be designed such that the pressure drops across each reagent inlet channel were equal. Such an arrangement allows the first two reagents to enter the first T-mixer simultaneously, and the resulting stream enters the second T-mixer at the same time as the

third inlet flow. This coalescence was confirmed by using FEMLAB simulations. At a flow rate of 15 μ L/min (5.8 min residence time), the simulations also showed that 90% of the mixing occurs within the first 15% of the mixing zone (3% of total residence time), ensuring fast mixing of the components.

Reaction times ranging from 1 to 30 min were controlled by adjusting the flow rate of the multihead syringe pump. The quench stream in the reactor is an important feature that sets finite and uniform reaction times for the sequential reactions. Temperatures ranging from -30 to 100 °C were achieved by using the thermoelectric module and incorporating a sufficient heat sink. Collection of individual reaction pulses was achieved by coupling an optical trigger, an analytical scale switch, and a 96-well plate fraction collector. Analysis of the reaction screens was performed by UPLC/MS/ELSD.

Scaffold Synthesis. The synthesis of bicyclo[3.2.1]octanoid scaffolds derived from [5+2] cycloaddition of quinone monoketals and styrene derivatives was first reported by Büchi and co-workers in their work toward the synthesis of neolignan natural products.⁸ Further efforts resulted in an improved synthesis of bicyclo[3.2.1] derivatives.^{28,29} On the basis of these studies, we were able to develop optimized conditions for the synthesis of five bicyclo[3.2.1] substrates (Table 1) using carefully controlled addition of water. The relative stereochemistry of bicyclo[3.2.1] scaffold 7 was confirmed by X-ray crystallographic analysis.³⁰ The relative stereochemistry of bicyclo[3.2.1] substrates 8–11 was confirmed via ¹H coupling constants and 1D NOE analyses.³⁰

During reaction optimization, we observed that when rigorously water-free conditions were utilized for [5+2] cycloaddition of monoketal 1³¹ and styrene (Scheme 1), the major product was diene 12 rather than the desired bicyclo[3.2.1]octanoid 7. Ring-opened product 12 appears to arise from a retro-Dieckmann-type process with oxonium intermediate 13 and the methanol liberated during formation of oxonium intermediate 14.³² Addition of water effectively competes with methanol to preferentially afford the desired bicyclo[3.2.1]octanoid 7. However, the addition of >1 equiv of water resulted in competing hydrolysis of oxonium intermediate 14 affording benzoquinone 15. Reaction optimization revealed that the optimal amount of water needed in the reaction to maximize the yield of the desired bicyclo[3.2.1]octanoid 7 was 0.65 to 0.75 equiv.

Multidimensional Screening of Bicyclo[3.2.1]octanoid Scaffolds. The dense functionality of multifunctional bicyclo[3.2.1]octanoid scaffolds such as 7 and 9 is highly desirable for reaction discovery. With use of these scaffolds, 23 heteroatom nucleophiles, 16 carbon/dipole nucleophiles, and 16 electrophiles (reaction partners) were screened using the microfluidic platform (Figure 7). Due to the presence of multiple electrophilic centers on the substrate, reaction

(28) Collins, J. L.; Grieco, P. A.; Walker, J. K. *Tetrahedron Lett.* **1997**, *38*, 1321.

(29) For additional examples of [5+2] cycloadditions, see: (a) Engler, T. A.; Letavic, M. A.; Combrink, K. D.; Takusagawa, F. *J. Org. Chem.* **1990**, *55*, 5810. (b) Harmata, M.; Rashatasakhon, P. *Tetrahedron* **2003**, *59*, 2371.

(30) See the Supporting Information for complete experimental details.

(31) Clive, D. L.; Fletcher, S. P.; Liu, D. *J. Org. Chem.* **2004**, *69*, 3282.

(32) (a) Mak, C.-P.; Büchi, G. *J. Org. Chem.* **1981**, *46*, 1. (b) Maki, S.; Asaba, N.; Koremura, S.; Yamamura, S. *Tetrahedron Lett.* **1992**, *33*, 4169.

(26) Albrecht, J.; Jensen, K. F. *Electrophoresis* **2006**, *27*, 4960.

(27) Park, J.; Park, K.; Shin, K.; Park, H.; Kim, J.; Kim, R.; Park, S.; Song, Y. *Sens. Actuators, B* **2006**, *117*, 516.

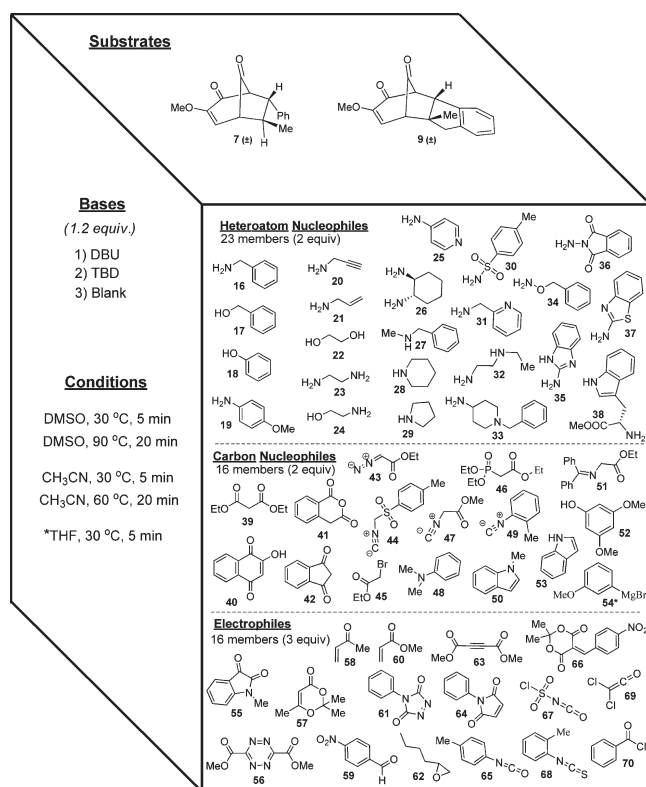


FIGURE 7. Multidimensional screening parameters.

partners capable of tandem nucleophilic additions (e.g., **22**, **23**, **24**, **26**, and **32**) were also included. Two non-nucleophilic bases 1,5,7-triazabicyclo[4.4.0]dec-5-ene (TBD) and 1,8-diazabicyclo[5.4.0]undec-7-ene (DBU), were utilized in the multidimensional screen. A complete representation of the screening dimensions is shown in Figure 7.

Each reaction was performed with 1 μ mol (typically 0.25 mg) of substrate, with 2.0 to 3.0 equiv of reaction partner and 1.2 equiv of base with a total reaction volume of 24 μ L. The latter volume was achieved by simultaneously delivering 8 μ L of each reaction component from stock solutions in the reagent storage block (Figure 3) to the reactor. The required stock solutions were prepared in both DMSO and CH₃CN in oven-dried glass sleeves with minimal exposure to air as 0.125 M solutions of the bicyclo[3.2.1] substrates, 0.250 M solutions of the reaction partners, and 0.150 M solutions of the bases.

Reaction times of 5 and 20 min were achieved by utilizing set flow rates of 4.5 and 1.2 μ L/min, respectively (multihead syringe pump with 4–10 mL syringes). Reactions were quenched in the reactor with 10% v/v acetic anhydride (continuous flow) and collected into 96-well plates by using UV-triggered fraction collection. The diluted reactions (final concentration = 1 mg/mL) were analyzed by using UPLC/MS/ELSD³³ without further preparation. Reactions affording > 20% conversion to a major product were subsequently scaled up and isolated by using traditional bench chemistry methods for further characterization of reaction products.

Analysis of UPLC/MS/ELSD data for the reaction screen indicated positive outcomes for 11 out of 23 heteroatom

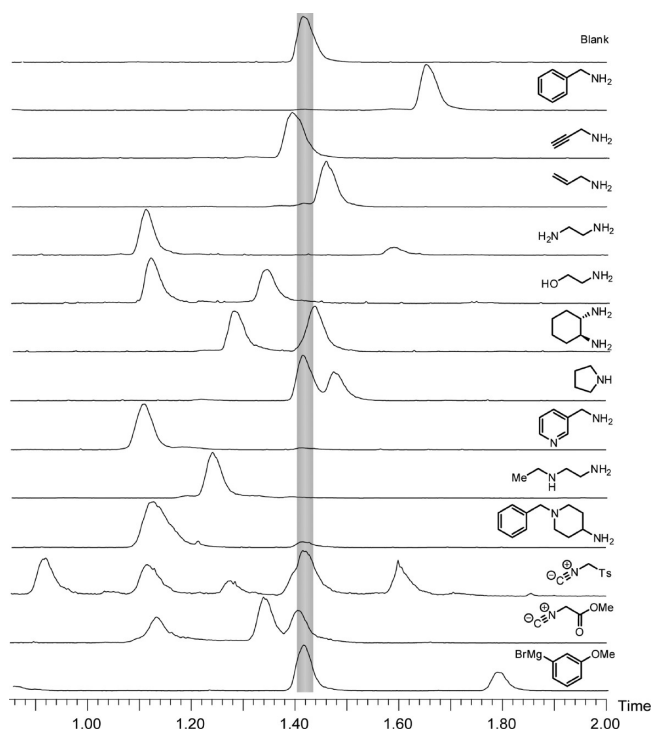


FIGURE 8. UPLC/ELSD results for successful transformations with bicyclo[3.2.1] substrate **7**. The shaded region represents the LC retention time for bicyclo[3.2.1] substrate **7**. Reaction conditions for displayed traces: DMSO, TBD, 5 min, 30 °C.

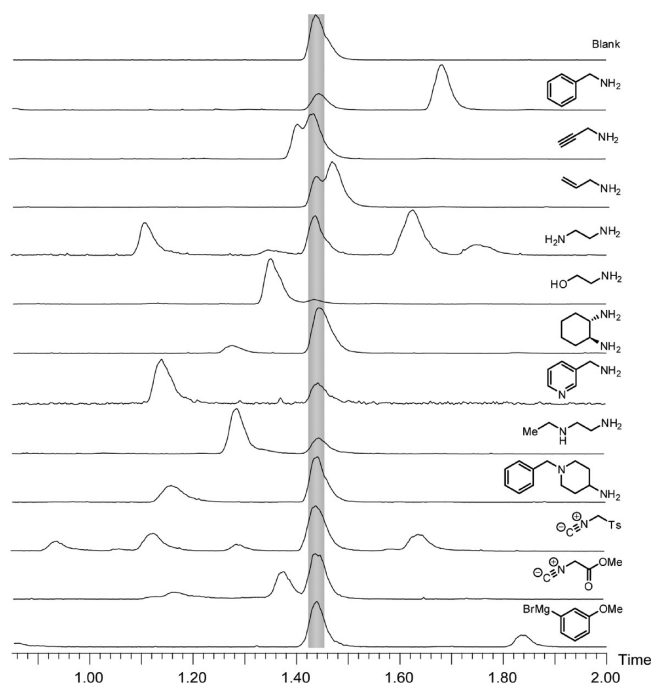
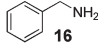
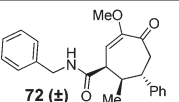
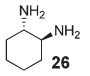
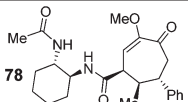
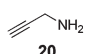
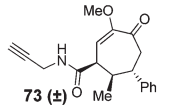
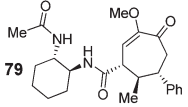
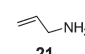
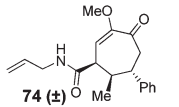
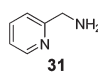
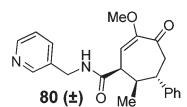
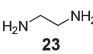
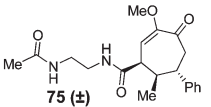
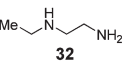
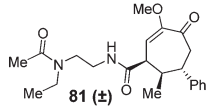
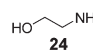
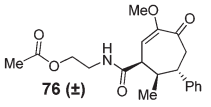
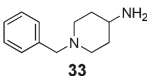
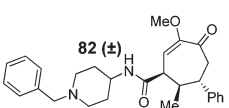
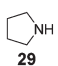
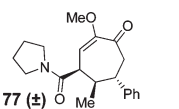
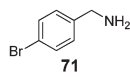
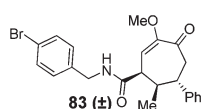


FIGURE 9. UPLC/ELSD results for successful transformations with bicyclo[3.2.1] substrate **9**. The shaded area represents the LC retention time for bicyclo[3.2.1] substrate **9**. Reaction conditions for displayed traces: CH₃CN, TBD, 5 min, 30 °C.

nucleophiles (Figures 8 and 9). All primary amine nucleophiles afforded retro-Dieckmann-type ring-opened products **72–93** (Tables 2 and 3). Although positive results utilizing

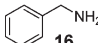
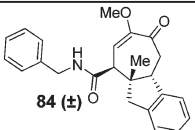
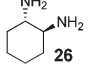
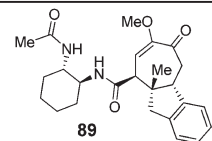
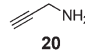
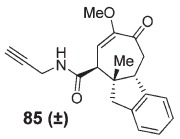
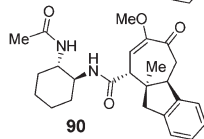
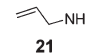
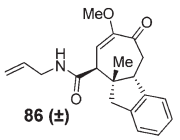
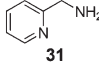
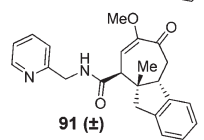
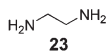
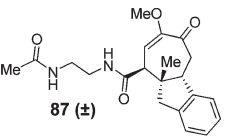
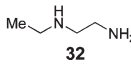
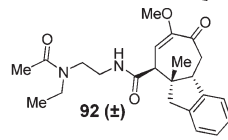
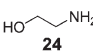
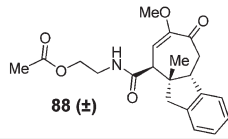
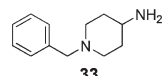
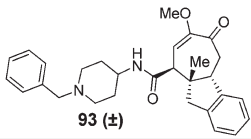
(33) Mazzeo, J. R.; Neue, U. D.; Kele, M.; Plumb, R. S. *Anal. Chem.* **2005**, *77*, 460 A.

TABLE 2. Results for Reactions with Bicyclo[3.2.1] Substrate 7^a

entry	nucleophile	product	yield (dr)	entry	nucleophile	product	yield (dr)
1			63 % ^b (20:1)	7			35 % ^c (>25:1)
2			60 % (11:1)				23 % ^c (>25:1)
3			54 % (13:1)	8			55 % (>20:1)
4			65 % ^c (14:1)	9			40 % (10:1)
5			57 % (10:1)	10			63 % (>25:1)
6			56 % ^d (9:1)	11			65 % (>25:1)

^aReaction conditions: nucleophile (2 equiv), DBU (1.2 equiv), anhydrous CH₃CN, room temperature, 1 h. ^bTBD (1.2 equiv): 50% yield (8:1). ^cNucleophile (12 equiv). ^dTBD (1.2 equiv).

TABLE 3. Results for Reactions with Bicyclo[3.2.1] Substrate 9^a

entry	nucleophile	product	yield (dr)	entry	nucleophile	product	yield (dr)
1			72 % (7:1)	6			27 % ^b (>25:1)
2			65 % (8:1)				24 % ^b (>25:1)
3			76 % (7:1)	7			64 % (8:1)
4			53 % ^b (9:1)	8			54 % (5:1)
5			68 % (10:1)	9			49 % (>25:1)

^aReaction conditions: nucleophile (2 equiv), TBD (1.2 equiv), anhydrous CH₃CN, room temperature, 1 h. ^bNucleophile (12 equiv).

bicyclo[3.2.1] substrate **7** were observed when either DBU or TBD was used, higher rates of conversion were generally observed by using the latter base. Interestingly, positive results utilizing substrate **9** were only observed when TBD was used as base.

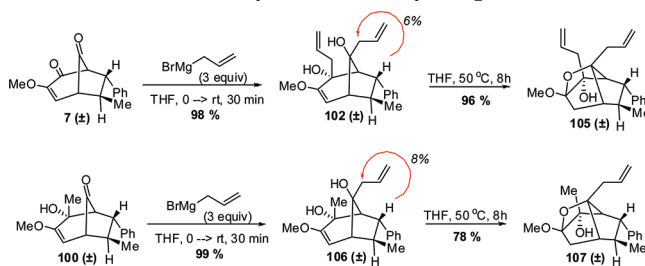
During scale-up and optimization of ring-opened products such as product **72**, it became apparent that epimerization of the α -amide stereocenter was occurring, giving rise to the isolation of a mixture of diastereomers (Tables 2 and 3). It was also noted that greater rates of epimerization occurred with the stronger base, TBD, which is expected given a predicted pK_a of ~ 25 for the α -amide proton.³⁴ Thus, the observed diastereomeric ratios reported in Tables 2 and 3 are primarily dictated by deprotonation kinetics, which are in part dependent on suitable alignment of the weakly acidic proton and the amide carbonyl. The relative stereochemistry of the major diastereomer of amide **83** was confirmed by X-ray crystallographic analysis.³⁰ Conformational analysis followed by *ab initio* (B3LYP, 6-31g*) minimization of both possible diastereomers of amides **72**, **77**, and **82** indicated that the major diastereomers are thermodynamically favored by approximately 1–2 kcal/mol.³⁰ These data indicate that while epimerization is under kinetic control, a thermodynamic equilibrium may exist favoring the initially formed diastereomer (cf. **72**–**93**).

Heteroatom nucleophiles without an alkyl primary amine (e.g., benzyl alcohol, *p*-anisidine, phenol, and *O*-benzylhydroxylamine) did not react under any of the conditions examined in the screen. This is attributed to the lower nucleophilicity of these reaction partners in comparison to those containing a primary alkyl amine. Similarly, secondary amines (e.g., *N*-methylbenzylamine, piperidine, and pyrrolidine) did not react. The only exception was the reaction between pyrrolidine (**29**) and bicyclo[3.2.1] substrate **7**, which afforded tertiary amide **77**.

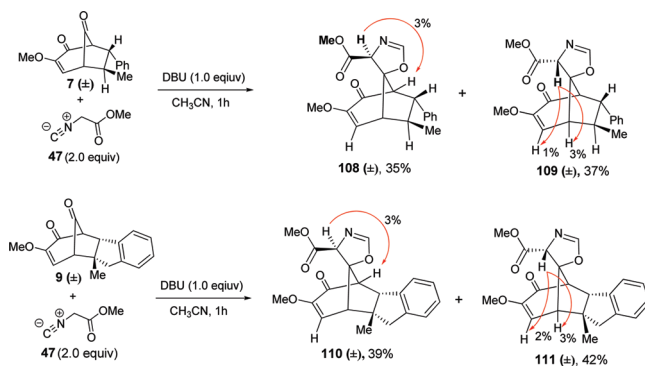
Reaction partners with the potential for tandem nucleophilic additions also afforded retro-Dieckmann-type ring-opened products, but did not undergo a second, intramolecular addition. As shown in Tables 2 and 3, the major isolated products were the acetylated amines and/or alcohols that were formed by quenching with acetic anhydride. While tandem addition products were not observed, tethered products were observed with diamino reaction partners **23** and **26**.³⁰ Increasing the amount of diamine to 12 equiv effectively prevented the formation of the tethered products. Utilization of chiral diamine **26** resulted in the formation of separable diastereomers (**78/79** and **89/90**). The absolute stereochemistry of **89** was confirmed by X-ray crystallographic analysis.³⁰ The relative stereochemistries of **78**, **79**, and **90** were assigned by using NMR analysis.

UPLC/MS/ELSD analysis of the carbon nucleophile microfluidics screening (cf. Figure 7) also indicated positive outcomes for reactions with 3-methoxyphenylmagnesium bromide (**54**) and isonitriles **44** and **47** (Figures 8 and 9). Interestingly, structure elucidation of products derived from Grignard reagent **54** indicated that addition occurred at the enone carbonyl exclusively over the bridgehead ketone (Table 4). The addition afforded a single diastereomer, **98**,

SCHEME 2. Further Cyclization of Allyl Grignard Adducts



SCHEME 3. Representative Products for Isonitrile Reactions



with approach occurring opposite the phenyl group.³⁵ Related additions to bicyclo[3.2.1]octanoids have been reported; however, in these cases stereoselectivity was not observed.³⁶

To determine scope and limitation for this reaction, additional commercially available Grignard reagents were investigated using traditional bench chemistry methods. As shown in Table 4, Grignard reactions proceeded with excellent yield and afforded single diastereomers. Facial-selectivity for the addition to the diosphenol ether carbonyl was confirmed by X-ray crystallographic analysis of alcohol **100**.³⁰ As indicated in Table 4 (entry 5), only allyl magnesium bromide underwent a second addition to the bridgehead ketone to afford tertiary alcohol **102**. The relative stereochemistry of diol **102** was confirmed by 1D NOE analysis.³⁰ Furthermore, upon mild heating **102** underwent cyclization to afford polycyclic ketal **105** (Scheme 2).

Alcohol **100** derived from the addition of methyl Grignard was also treated with allyl magnesium bromide to afford diol **106**, which upon heating gave the polycyclic ketal **107**. Of the Grignard reagents investigated, only ethynyl Grignard (Table 4, entry 6) resulted in the formation of two regioisomers. In this case, addition to the enone carbonyl was still favored, but facially selective addition to the bridgehead ketone did occur. To confirm the relative stereochemistry of **104**, the tertiary alcohol was methylated by using standard conditions (NaH/MeI) to afford the corresponding methyl ether which was used to conduct 1D NOE analysis.^{30,37} Presumably, the smaller ethynyl functionality presents a

(36) Shizuri, Y.; Okuno, Y.; Shigemori, H.; Yamamura, S. *Tetrahedron Lett.* **1987**, *28*, 6661.

(37) For examples of *O*-methylation to obtain NOE correlations, see: (a) Komoda, T.; Sugiyama, Y.; Abe, N.; Imachi, M.; Hirota, H.; Koshino, H.; Hirota, A. *Tetrahedron Lett.* **2003**, *44*, 7417. (b) Najjar, F.; Baltas, M.; Gorrihon, L.; Moreno, Y.; Tzedakis, T.; Vail, H.; Andre-Barres, C. *Eur. J. Org. Chem.* **2003**, 3335.

(34) University of Wisconsin: Bordwell pK_a Table (Acidity in DMSO) <http://www.chem.wisc.edu/areas/reich/pkatable/> (accessed July 14, 2008).

(35) (a) Reetz, M. T. *Angew. Chem., Int. Ed. Engl.* **1984**, *23*, 556. (b) Ye, J.-L.; Huang, P.-Q.; Lu, X. *J. Org. Chem.* **2007**, *72*, 35.

TABLE 4. Results for Reactions with Grignard Additions^a

entry	sub	reagent	product	yield
1	7			96 %
2	9			99 %
3	7			95 %
4	7			91 %
5	7			98 %
6	7			60 %
				30 %

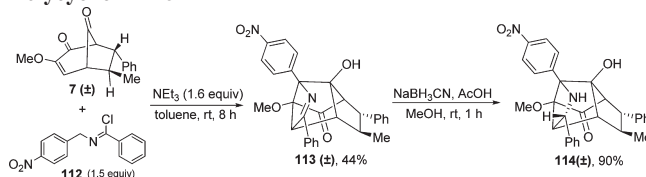
^aReaction conditions: Grignard reagent (3.0 equiv), anhydrous THF, 0 °C → rt, 30 min.

smaller steric profile than the other Grignard reagents investigated and thus is able to approach the bridgehead ketone from the less hindered face bearing the α -methoxy enone.

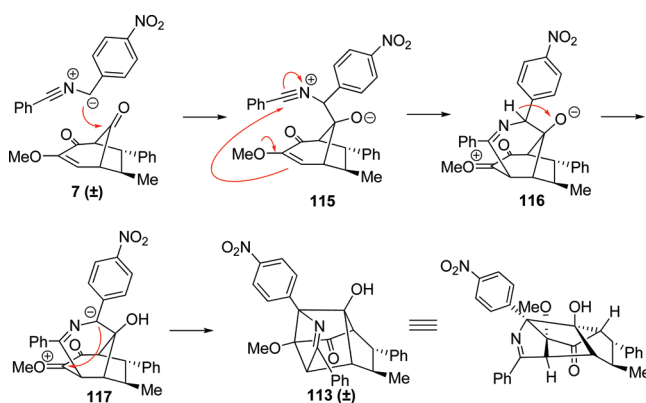
Elucidation of the successful microfluidics reactions of bicyclo[3.2.1] substrates **7** and **9** with isonitriles **44** and **47** revealed that a [3+2] cycloaddition had occurred at the bridgehead ketone³⁸ in a 1:1 diastereomeric ratio affording spirooxazolines **108** and **109** (Scheme 3). Diastereoselectivity of the cycloaddition occurs through addition to the less hindered face bearing the α -methoxy enone. These structural assignments were supported by 1D NOE analyses (Scheme 2).^{30,39} The spirooxazolines **108**–**111** were found to be prone to hydrolysis, affording ring-opened formamides.^{39a} Reaction products derived from *p*-toluenesulfonyl methyl isocyanide (**44**) suffered significant decomposition while on silica and could not be cleanly isolated.

Interestingly, when an isocyanide lacking an α -acidic proton (**49**) was utilized, no reaction occurred. This suggests that the formation of an isonitrile ylide intermediate^{39a} in the presence of base is a critical step in this process. On the basis

SCHEME 4. Condensation with an Isonitrile Ylide Affords a Polycyclic Imine



SCHEME 5. Proposed Mechanism for the Formation of Polycyclic Imine **113**



of this observation, we investigated an additional nitrile ylide using a standard batch reaction (Scheme 4).⁴⁰ Structure elucidation of the isolated product revealed formation of the unusual polycyclic imine **113**. The structure was confirmed by X-ray crystallographic analysis.³⁰ Selective reduction of the imine with NaBH₃CN and acetic acid afforded **114** as a single diastereomer.⁴¹

A proposed mechanism for the formation of imine **113** is shown in Scheme 5 and takes advantage of the proximity of the diosphenol ether and bridgehead ketone on the bicyclo[3.2.1]octanoid scaffold. Addition of the dipole to the bridgehead ketone generates the nitrilium zwitterion **115**.⁴² The enol ether may then undergo intramolecular addition to the emerged nitrilium to afford oxonium intermediate **116**. Base-mediated proton transfer generates a new zwitterion **117** that undergoes intramolecular cyclization to afford **113**.

Finally, UPLC/MS/ELSD analyses of the electrophile reaction partner subset did not reveal any successful transformations. The lack of reactivity with the electrophiles was unexpected given the participation of the diosphenol ether moiety observed in the formation of polycyclic imine **113**.

Conclusion

A microfluidic reaction platform has been developed and used for multidimensional reaction screening of highly functionalized bicyclo[3.2.1]octanoid scaffolds. This

(38) For examples of dipole additions to bridgehead ketones see: (a) Van Leusen, D.; Van Leusen, A. M. *Org. React.* **2001**, *57*, 417. (b) Groselj, U.; Meden, A.; Stanovnik, B.; Svetec, J. *Tetrahedron: Asymmetry*. **2007**, *18*, 2365.

(39) For examples of cycloadditions with isonitriles, see: (a) Soloshonok, V. A.; Kacharov, A. D.; Avilov, D. V.; Ishikawa, K.; Nagashima, N.; Hayashi, T. *J. Org. Chem.* **1997**, *62*, 3470. (b) Terzidis, M.; Tsoerlidis, C. A.; Stephanidou-Stephanatou, J. *Tetrahedron* **2007**, *63*, 7828.

(40) Nair, V.; Sethumadhaven, D.; Nair, S. M.; Viji, S.; Rath, N. P. *Tetrahedron* **2002**, *58*, 3003.

(41) Kiss, L.; Mangelinckx, S.; Fulop, F.; De Kiimpe, N. *Org. Lett.* **2007**, *9*, 4399.

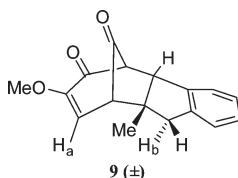
(42) For examples of stepwise cycloaddition, see: (a) Cantillo, D.; Avalos, D.; Babiano, R.; Cintas, P.; Jimenez, J. L.; Light, M. E.; Palacios, J. C. *Org. Lett.* **2008**, *10*, 1079. (b) Deng, X.; Mani, N. S. *Org. Lett.* **2008**, *10*, 1307. (c) Xie, J.; Yoshida, K.; Takasu, K.; Takemoto, Y. *Tetrahedron Lett.* **2008**, *49*, 6910. (d) Shapiro, N. D.; Toste, F. D. *J. Am. Chem. Soc.* **2008**, *130*, 9244.

study represents a successful application of microfluidics technology to reaction discovery allowing for over 1000 reactions to be screened and analyzed on an analytical scale. Use of the microfluidic platform enabled expansion of an interesting retro-Dieckmann-type fragmentation affording highly functionalized cycloheptenone derivatives. Furthermore, [3+2] cycloaddition involving the bridgehead ketone of the bicyclo[3.2.1]octanoid scaffolds and isocyanides was observed in the reaction screen. These dipole cycloadditions inspired the ultimate discovery of a stepwise condensation of an isonitrile ylide to afford a novel polycyclic imine. Finally, use of moisture-sensitive Grignard reagents with the microfluidics platform resulted in the discovery of chemo- and stereoselective additions to the bicyclo[3.2.1]octanoid scaffolds, highlighting the overall reagent capability of the screening platform. Additional applications of microfluidics-enabled multidimensional reaction screening and expansion of the platform capabilities for reaction optimization and scaleup are currently underway and will be reported in due course.

Experimental Section

(1*R*,5*R*,6*R*,7*R*)-3-methoxy-6-methyl-7-phenylbicyclo[3.2.1]-oct-3-ene-2,8-dione (±)-7. To an oven-dried vial was added dry (1*S*)-(+)-10-camphorsulfonic acid (CSA) (63 mg, 0.27 mmol) followed by anhydrous CH₃CN (3 mL), water (3.7 μL, 0.21 mmol), and β-*trans*-methylstyrene (70 μL, 0.54 mmol). To this mixture was added 3,4,4-trimethoxycyclohexa-2,5-dienone (50 mg, 0.27 mmol) dissolved in CH₃CN (1 mL). The reaction was stirred at rt for 1.5 h, quenched with triethylamine (38 μL), and stirred for 15 min. The solution was diluted with sat. NaHCO₃ and extracted with diethyl ether (3×). The organic layer was washed with brine (1×), dried over sodium sulfate, filtered, and evaporated *in vacuo*. The crude material was purified by flash chromatography (SiO₂, 20:80 EtOAc:petroleum ether) to afford **3** (43%, 66 mg, 0.27 mmol) as clear/white crystals. Mp 140–142 °C; ¹H NMR (400 MHz, CDCl₃) δ 7.31–7.25 (m, 2 H), 7.24–7.19 (m, 1 H), 7.05 (d, *J* = 8.6 Hz, 2 H), 6.48 (d, *J* = 8.6 Hz, 1 H), 3.81 (dd, *J* = 7.0, 2.0 Hz, 1 H), 3.72 (s, 3 H), 3.20 (t, *J* = 6.5 Hz, 1 H), 3.05 (dd, *J* = 8.6, 2.1 Hz, 1 H), 2.56 (qt, *J* = 6.7 Hz, 1 H), 1.26 (d, *J* = 7.0 Hz, 3 H); ¹³C NMR (100 MHz, CDCl₃) δ 200.2, 190.3, 154.6, 138.0, 129.1, 128.6, 127.8, 118.1, 71.1, 56.0, 54.1, 49.6, 43.2, 21.7; IR (thin film) ν_{max} 2962, 1761, 1684, 1606, 1456, 1363, 1245, 1223, 1153, 1103, 1036, 753, 701 cm⁻¹; HRMS calcd for C₁₆H₁₆O₃Na 279.0997, found 279.1022 (M + Na).

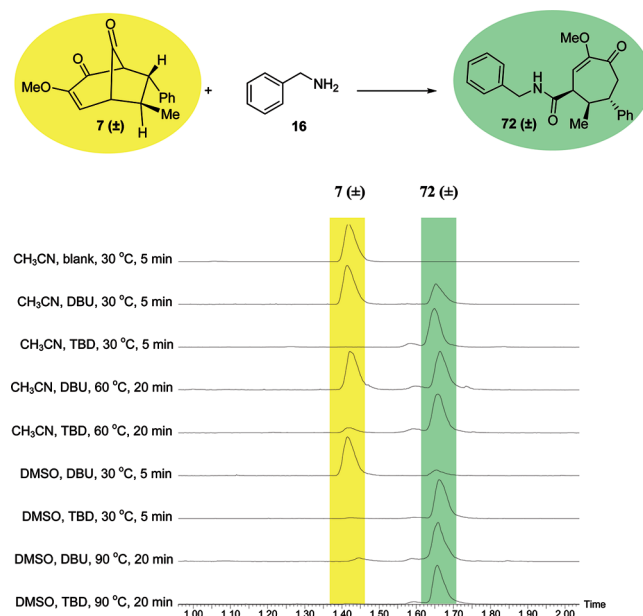
Bicyclo[3.2.1]octanoid (±)-9.



To an oven-dried vial was added dry (1*S*)-(+)-10-camphorsulfonic acid (CSA) (63 mg, 0.27 mmol) followed by anhydrous CH₃CN (3 mL), water (3.7 μL, 0.21 mmol), and 2-methylindene (73 μL, 0.54 mmol). To this mixture was added 3,4,4-trimethoxycyclohexa-2,5-dienone (50 mg, 0.27 mmol) dissolved in CH₃CN (1 mL). The reaction was stirred at rt for 1.5 h, quenched with triethylamine (38 μL), and stirred for 15 min. The solution was diluted with sat. NaHCO₃ and extracted with diethyl ether (3×). The organic layer was washed with

brine (1×), dried over sodium sulfate, filtered, and evaporated *in vacuo*. The crude material was purified by flash chromatography (SiO₂, 20:80 EtOAc:petroleum ether) to afford **9** (70%, 51 mg, 0.19 mmol) as clear/white crystals; mp 135–138 °C; ¹H NMR (400 MHz, CDCl₃) δ 7.17–7.10 (m, 2 H), 7.09–7.03 (m, 2 H), 6.04 (d, *J* = 8.3 Hz, 1 H), 4.02 (dd, *J* = 8.3, 1.8 Hz, 1 H), 3.77 (d, *J* = 8.3 Hz, 1 H), 3.35 (s, 3 H), 3.20 (d, *J* = 17.3 Hz, 1 H), 3.12 (dd, *J* = 8.3, 2.0 Hz, 1 H), 2.95 (d, *J* = 17.3 Hz, 1 H), 1.42 (s, 3 H); NOED (400 MHz, CDCl₃) irradi. δ 6.04 (H_a) 2% enhancement at H_b, irradi. δ 3.20 (H_b) 3% enhancement at H_a; ¹³C NMR (100 MHz, CDCl₃) δ 200.5, 190.3, 154.7, 143.8, 140.1, 128.0, 127.5, 126.2, 124.1, 114.2, 67.5, 58.1, 55.8, 55.1, 47.2, 42.5, 28.4; IR (thin film) ν_{max} 2962, 2923, 1762, 1685, 1608, 1458, 1218, 1141, 749 cm⁻¹; HRMS calcd for C₁₇H₁₆O₃Na 291.0997, found 291.1026 (M + Na).

General Procedure for Analytical Reaction Screening (Automated Microfluidics Platform). Stock solutions of substrate (0.125 M), reaction partner (0.25 M), and base (0.15 M) were prepared in DMSO or CH₃CN (anhydrous) while maintaining dry handling. The solutions were placed in a custom-designed 96-well aluminum holding block fitted with oven-dried glass sleeves. This was covered with an inert gas chamber and sealed. The block was attached to the microfluidics platform and a slow steady stream of argon was passed through the inert gas chamber. System parameters were first set to achieve 5 min reactions (microreactor residence time) at 30 °C. Longer reaction times at elevated reaction temperatures were achieved by decreasing the syringe pump flow rate and increasing the power supply to the TE heating module. Reactions were quenched on the microreactor by flowing acetic anhydride (10% V/V in DMSO or CH₃CN) into the quench port. Individual reactions were collected into 96-well plates with use of optical detection. Each reaction was analyzed by UPLC/MS/ELSD (10–90% CH₃CN, 2 min). Reactions affording > 20% conversion to a major product were subsequently scaled up and isolated, using traditional bench chemistry methods, for further characterization. A sample UPLC/ELSD profile for substrate **7** and benzylamine (**16**) is provided below.



(1*R*,6*S*,7*R*,*E*)-*N*-Benzyl-3-methoxy-7-methyl-4-oxo-6-phenylcyclohept-2-enecarboxamide (±)-72. To an oven-dried 1-dram

vial was added 3-methoxy-6-methyl-7-phenylbicyclo[3.2.1]oct-3-ene-2,8-dione (**7**) (40 mg, 0.16 mmol) and anhydrous CH₃CN (0.90 mL) followed by the addition of benzylamine (34 μ L, 0.31 mmol). To this mixture was added DBU (28 μ L, 0.19 mmol) in anhydrous CH₃CN (100 μ L). The reaction was stirred at rt for 60 min under argon and quenched with the addition of acetic anhydride (44 μ L, 0.47 mmol) in CH₃CN (400 μ L). The reaction was filtered through a short plug of silica and washed with CH₃CN (3 \times 2 mL, until all the product was eluted from the silica plug as indicated by TLC). The eluent was then evaporated *in vacuo*. The crude material was purified by flash chromatography (SiO₂, 40:1 CH₂Cl₂:MeOH) to afford **72** as a mixture of diastereomers in 20:1 ratio (dr was estimated from crude UPLC/ELSD) (63%, 36 mg, 0.098 mmol). Characterization data for the major diastereomer: ¹H NMR (400 MHz, CDCl₃) δ 7.37–7.21 (m, 8 H), 7.17–7.12 (m, 2 H), 6.20 (d, J = 6.1 Hz, 1 H), 5.95 (t, J = 5.3 Hz, 1 H), 4.50 (dd, J = 5.5, 4.1 Hz, 2 H), 3.73 (s, 3 H), 3.71 (ovrlp t, J = 5.7 Hz, 1 H), 3.02 (dd, J = 17.6, 11.9 Hz, 1 H), 2.80 (dd, J = 17.6, 1.2 Hz, 1 H), 2.60 (dd, J = 11.1, 9.8 Hz, 1 H), 2.26–2.14 (m, 1 H), 0.88 (d, J = 6.6 Hz, 3 H); ¹³C NMR (100 MHz, CDCl₃) δ 197.3, 171.2, 152.8, 143.8, 137.9, 128.8, 128.7, 128.0, 127.7, 126.9, 107.6, 55.5, 48.1, 45.9, 45.0, 44.1, 43.0, 15.3; IR (thin film) ν_{\max} 3337, 2961, 2927, 1666, 1537, 1454, 1345, 1208, 1140, 701 cm⁻¹; HRMS calcd for C₂₃H₂₆NO₃ 364.1913, found 364.1937 (M + H).

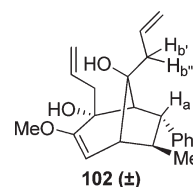
(**1R,6S,7R,E**)-*N*-(4-Methoxybenzyl)-3-methoxy-7-methyl-4-oxo-6-phenylcyclohept-2-enecarboxamide (\pm)-**77**. To an oven-dried 1-dram vial was added 3-methoxy-6-methyl-7-phenylbicyclo[3.2.1]oct-3-ene-2,8-dione (**7**) (40 mg, 0.16 mmol) and anhydrous CH₃CN (0.90 mL) followed by the addition of pyrrolidine (26 μ L, 0.31 mmol). To this mixture was added TBD (26 mg, 0.19 mmol) in anhydrous CH₃CN (100 μ L). The reaction was stirred at rt for 60 min under argon and quenched with the addition of acetic anhydride (44 μ L, 0.47 mmol) in CH₃CN (400 μ L). The reaction was filtered through a short plug of silica and washed with CH₃CN (3 \times 2 mL, until all the product was eluted from the silica plug as indicated by TLC). The eluent was then evaporated *in vacuo*. The crude material was purified by flash chromatography (SiO₂, 40:1 CH₂Cl₂:MeOH) to afford **77** as a mixture of diastereomers in 9:1 ratio (dr was estimated from crude UPLC/ELSD) (56%, 29 mg, 0.087 mmol). Characterization data for the major diastereomer: ¹H NMR (400 MHz, CDCl₃) δ 7.36–7.22 (m, 3 H), 7.16 (d, J = 7.4 Hz, 2 H), 6.25 (d, J = 5.9 Hz, 1 H), 3.98 (t, J = 5.5 Hz, 1 H), 3.73 (s, 3 H), 3.67–3.40 (m, 4 H), 3.07 (dd, J = 17.6, 12.5 Hz, 1 H), 2.83 (d, J = 17.6 Hz, 1 H), 2.61 (dd, J = 11.7, 9.4 Hz, 1 H), 2.31–2.18 (m, 1 H), 2.06–1.97 (m, 2 H), 1.93–1.85 (m, 2 H), 0.88 (d, J = 6.6 Hz, 3 H); ¹³C NMR (100 MHz, CDCl₃) δ 197.3, 170.1, 152.6, 144.2, 128.8, 127.6, 126.8, 109.2, 55.5, 48.1, 46.5, 46.0, 43.0, 40.3, 26.3, 24.1, 15.5; IR (thin film) ν_{\max} 2966, 1728, 1680, 1625, 1452, 1209, 1137, 733, 703 cm⁻¹; HRMS calcd for C₂₀H₂₅NO₃Na 350.1732, found 350.1714 (M + Na).

(**1R,6S,7R,E**)-*N*-(4-Methoxybenzyl)-3-methoxy-7-methyl-4-oxo-6-phenylcyclohept-2-enecarboxamide (\pm)-**84**. To an oven-dried 1-dram vial was added bicyclo[3.2.1]octanoid **9** (40 mg, 0.15 mmol) and anhydrous CH₃CN (0.90 mL) followed by the addition of benzylamine (30 μ L, 0.30 mmol). To this mixture was added TBD (25 mg, 0.18 mmol) in anhydrous CH₃CN (100 μ L). The reaction was stirred at rt for 60 min under argon and quenched with the addition of acetic anhydride (42 μ L, 0.45 mmol) in CH₃CN (400 μ L). The reaction was filtered through a short plug of silica and washed with CH₃CN (3 \times 2 mL, until all the product was eluted from the silica plug as indicated by TLC). The eluent was then evaporated *in vacuo*. The crude material was purified by flash chromatography (SiO₂, 40:1 CH₂Cl₂:MeOH) to afford **84** as a mixture of diastereomers in 7:1 ratio (dr was estimated from crude UPLC/ELSD) (72%, 40 mg, 0.11 mmol). Characterization data for the major diastereomer: ¹H NMR (400 MHz, CDCl₃) δ 7.44–7.30 (m, 5 H), 7.20 (d, J = 4.3 Hz, 3

H), 7.14 (br s, 1 H), 6.14 (d, J = 5.9 Hz, 1 H), 5.96 (t, J = 5.1 Hz, 1 H), 4.60 (dd, J = 14.5, 5.5 Hz, 1 H), 4.52 (dd, J = 14.5, 5.5 Hz, 1 H), 3.70 (s, 3 H), 3.40 (d, J = 5.9 Hz, 1 H), 3.06 (d, J = 15.6 Hz, 1 H), 2.98 (dd, J = 11.7, 2.7 Hz, 1 H), 2.77–2.68 (m, 3 H), 1.15 (s, 3 H); ¹³C NMR (100 MHz, CDCl₃) δ 196.3, 171.3, 153.1, 143.3, 141.1, 137.9, 128.8, 128.0, 127.8, 127.4, 127.2, 124.9, 124.8, 111.9, 55.4, 51.0, 50.6, 48.7, 46.6, 44.4, 44.2, 23.4; IR (thin film) ν_{\max} 3334, 2930, 1673, 1622, 1537, 1455, 1206, 1155, 1137, 1119, 754, 734, 700 cm⁻¹; HRMS calcd for C₂₄H₂₆NO₃ 376.1913, found 376.1919 (M + H).

(**1R,4S,5S,6R,7R**)-4-Hydroxy-3-methoxy-4-(3-methoxyphenyl)-7-methyl-6-phenylbicyclo[3.2.1]oct-2-en-8-one (\pm)-**98**. To an oven-dried vial was added 3-methoxy-6-methyl-7-phenylbicyclo[3.2.1]oct-3-ene-2,8-dione (**7**) (40 mg, 0.16 mmol) and anhydrous THF (4.0 mL). The reaction mixture was cooled to 0 °C while under argon. To this mixture was added 1.0 M 3-methoxyphenylmagnesium bromide in THF (470 μ L, 0.47 mmol) dropwise via syringe over 1 min while at 0 °C. The reaction was warmed to rt with continued stirring for 30 min. The reaction was cooled back down to 0 °C and quenched with the addition of water (20 μ L). This mixture was warmed to rt, diluted with water (20 mL), and extracted into CH₂Cl₂ (3 \times 15 mL). The organic fractions were combined, washed with brine (20 mL), dried over sodium sulfate, filtered, and evaporated *in vacuo*. The crude product was purified by flash chromatography (SiO₂, 40:1 CH₂Cl₂:EtOAc) to afford **98** as an amorphous clear/white solid (96%, 54 mg, 0.15 mmol). ¹H NMR (400 MHz, CDCl₃) δ 7.46–7.36 (m, 4 H), 7.33–7.27 (m, 1 H), 7.21–7.15 (m, 1 H), 6.83–6.81 (m, 1 H), 6.80–6.74 (m, 2 H), 5.39 (d, J = 7.4 Hz, 1 H), 3.74 (s, 3 H), 3.64 (s, 3 H), 3.09 (dd, J = 7.0, 5.9 Hz, 1 H), 2.94 (dd, J = 7.0, 1.6 Hz, 1 H), 2.88–2.78 (m, 1 H), 2.58 (dd, J = 7.4, 1.6 Hz, 1 H), 2.09 (s, 1 H), 1.07 (d, J = 7.0 Hz, 3 H); ¹³C NMR (100 MHz, CDCl₃) δ 205.7, 159.4, 155.4, 144.1, 140.6, 129.5, 128.8, 128.8, 127.2, 118.1, 113.2, 111.6, 99.5, 82.7, 63.6, 55.3, 55.1, 51.2, 50.4, 42.7, 21.5; IR (thin film) ν_{\max} 3552, 2958, 1750, 1600, 1584, 1484, 1455, 1434, 1289, 1250, 1227, 1150, 1095, 1079, 1032, 784, 701 cm⁻¹; HRMS calcd for C₂₃H₂₄O₄Na 387.1572, found 387.1587 (M + Na).

(**1R,2R,5R,6R,7R,8S**)-2,8-Diallyl-3-methoxy-6-methyl-7-phenylbicyclo[3.2.1]oct-3-ene-2,8-diol (\pm)-**102**.

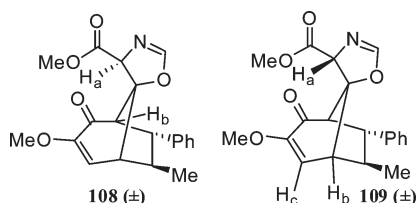


To an oven-dried vial was added 3-methoxy-6-methyl-7-phenylbicyclo[3.2.1]oct-3-ene-2,8-dione (**7**) (40 mg, 0.16 mmol) and anhydrous THF (4.0 mL). The reaction mixture was cooled to 0 °C while under argon. To this mixture was added 1.0 M allylmagnesium bromide in diethyl ether (470 μ L, 0.47 mmol) dropwise via syringe over 1 min while at 0 °C. The reaction was warmed to rt with continued stirring for 30 min. The reaction was cooled back down to 0 °C and quenched with the addition of water (20 μ L). This mixture was warmed to rt, diluted with water (20 mL), and extracted into CH₂Cl₂ (3 \times 15 mL). The organic fractions were combined, washed with brine (20 mL), dried over sodium sulfate, filtered, and evaporated *in vacuo*. The crude product was purified by flash chromatography (SiO₂, 40:1 CH₂Cl₂:EtOAc) to afford **102** as an amorphous clear/white solid (98%, 52 mg, 0.15 mmol). ¹H NMR (400 MHz, CDCl₃) δ 7.32–7.22 (m, 4 H), 7.20–7.13 (m, 1 H), 6.12–5.98 (ddt,

$J = 17.2, 10.1, 7.2$ Hz, 1 H), 5.91–5.77 (ddt, $J = 17.4, 10.2, 7.1$ Hz, 1 H), 5.25–5.03 (m, 5 H), 3.56 (s, 3 H), 3.35 (dd, $J = 9.2, 5.8$ Hz, 1 H), 2.82 (dd, $J = 5.8, 2.0$ Hz, 1 H), 2.79–2.67 (ovrlp m, 2 H), 2.64 (d, $J = 7.4$ Hz, 2 H), 2.60–2.52 (m, 1 H), 2.38 (s, 1 H), 2.18 (dd, $J = 7.8, 2.0$ Hz, 1 H), 1.28 (s, 1 H), 1.18 (d, $J = 7.0$ Hz, 3 H); NOED (400 MHz, CDCl_3) irradi. δ 3.35 (H_a) 7% enhancement at H_b' , 5% enhancement at H_b'' ; ^{13}C NMR (100 MHz, CDCl_3) δ 160.0, 141.5, 134.7, 134.0, 128.7, 126.1, 118.5, 118.1, 99.8, 81.5, 77.6, 55.0, 53.2, 51.4, 49.1, 43.8, 43.4, 42.6, 20.6; IR (thin film) ν_{max} 3566, 2954, 2928, 1638, 1450, 1373, 1223, 1153, 1065, 1033, 999, 912, 697 cm^{-1} ; HRMS calcd for $\text{C}_{22}\text{H}_{28}\text{O}_3\text{Na}$ 363.1936, found 363.1942 (M + Na).

Polycyclic Ketal (\pm)-105. To a 1-dram vial was added diol **102** (20 mg, 0.059 mmol) followed by the addition of THF (1 mL). The reaction mixture was heated to 50 °C for 8 h while stirring. The reaction was concentrated and purified by flash chromatography (SiO_2 , 40:1 CH_2Cl_2 :EtOAc) to afford **105** as an amorphous clear/white solid (96%, 19 mg, 0.056 mmol). ^1H NMR (400 MHz, CDCl_3) δ 7.31–7.27 (m, 4 H), 7.21–7.14 (m, 1 H), 6.02–5.89 (m, 1 H), 5.61–5.48 (m, 1 H), 5.20–5.12 (m, 2 H), 4.98–4.89 (m, 2 H), 3.45 (s, 3 H), 2.91 (dd, $J = 9.6, 5.7$ Hz, 1 H), 2.83–2.71 (m, 1 H), 2.59 (d, $J = 7.0$ Hz, 2 H), 2.48 (dd, $J = 5.7, 1.6$ Hz, 1 H), 2.32–2.14 (ovrlp m, 3 H), 2.07–1.96 (ovrlp m, 2 H), 1.24 (s, 1 H), 1.14 (d, $J = 7.0$ Hz, 3 H); ^{13}C NMR (100 MHz, CDCl_3) δ 140.0, 133.6, 133.4, 128.2, 128.1, 125.9, 119.7, 117.7, 109.7, 89.1, 81.4, 56.0, 52.5, 50.9, 49.5, 41.6, 40.6, 38.1, 36.2, 22.3; IR (thin film) ν_{max} 2953, 1498, 1456, 1447, 1311, 1217, 1154, 1134, 1096, 1064, 1032, 994, 912, 697 cm^{-1} ; HRMS calcd for $\text{C}_{22}\text{H}_{28}\text{O}_3\text{Na}$ 363.1936, found 363.1944 (M + Na).

(1R,4S,5R,5'R,6R,7R)-Methyl 3-Methoxy-7-methyl-4-oxo-6-phenyl-4'H-spiro[bicyclo[3.2.1]oct[2]ene-8,5'-oxazole]-4'-carboxylate (\pm)-108 and (1R,4'R,5R,5'R,6R,7R)-Methyl 3-Methoxy-7-methyl-4-oxo-6-phenyl-4'H-spiro[bicyclo[3.2.1]oct[2]ene-8,5'-oxazole]-4'-carboxylate (\pm)-109.

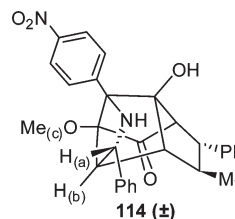


To an oven-dried 1-dram vial was added 3-methoxy-6-methyl-7-phenylbicyclo[3.2.1]oct-3-ene-2,8-dione (**7**) (40 mg, 0.16 mmol) and anhydrous CH_3CN (0.90 mL) followed by the addition of isocyanoacetate (28.3 μL , 0.312 mmol). To this mixture was added DBU (28 μL , 0.19 mmol) in anhydrous CH_3CN (100 μL). The reaction was stirred at rt for 60 min under argon, quenched by filtering through a short plug of silica, and washed with CH_3CN (3×2 mL, until all the product was eluted from the silica plug as indicated by TLC). The eluent was then evaporated *in vacuo*. The crude material was purified by flash chromatography (SiO_2 , 1:1 EtOAc:petroleum ether) to afford **108** (35%, 19 mg, 0.055 mmol) and **109** (37%, 21 mg, 0.058 mmol) as amorphous clear/white solids. Characterization data for **108**: ^1H NMR (400 MHz, CDCl_3) δ 7.29–7.22 (m, 2 H), 7.22–7.14 (m, 1 H), 7.08–7.00 (m, 3 H), 6.26 (d, $J = 8.2$ Hz, 1 H), 4.48 (s, 1 H), 3.71 (s, 3 H), 3.62 (s, 3 H), 3.51 (t, $J = 6.4$ Hz, 1 H), 3.39 (dd, $J = 6.4, 2.0$ Hz, 1 H), 3.15 (dd, $J = 8.2, 2.0$ Hz, 1 H), 2.53 (quin, $J = 6.8$ Hz, 1 H), 1.35 (d, $J = 7.0$ Hz, 3 H); NOED (400 MHz, CDCl_3) irradi. δ 4.48 (H_a) 3% enhancement at H_b ; irradi. δ 3.39 (H_b) 2% enhancement at H_a ;

^{13}C NMR (100 MHz, CDCl_3) δ 192.0, 170.6, 156.2, 153.6, 138.0, 128.7, 128.3, 127.2, 121.2, 97.5, 70.9, 68.7, 55.4, 52.4, 51.4, 48.1, 46.6, 20.4; IR (thin film) ν_{max} 2955, 2932, 1743, 1696, 1635, 1616, 1456, 1251, 1212, 1159, 1113, 971, 736, 701 cm^{-1} ; HRMS calcd for $\text{C}_{20}\text{H}_{22}\text{NO}_5$ 356.1498, found 356.1513 (M + H). Characterization data for **109**: ^1H NMR (400 MHz, CDCl_3) δ 7.29–7.21 (m, 2 H), 7.21–7.14 (m, 1 H), 7.11 (s, 1 H), 7.02 (d, $J = 7.4$ Hz, 2 H), 6.28 (d, $J = 8.6$ Hz, 1 H), 4.67 (d, $J = 1.6$ Hz, 1 H), 3.72 (s, 3 H), 3.56 (s, 3 H), 3.56 (ovrlp t, $J = 6.45$ Hz, 1 H), 3.35 (dd, $J = 6.6, 2.3$ Hz, 1 H), 2.81 (dd, $J = 8.4, 2.1$ Hz, 1 H), 2.56 (d, $J = 7.0$ Hz, 1 H), 1.35 (d, $J = 7.0$ Hz, 3 H); NOED (400 MHz, CDCl_3) irradi. δ 4.67 (H_a) 3% enhancement at H_b , 1% enhancement at H_c ; irradi. δ 2.81 (H_b) 2% enhancement at H_a ; ^{13}C NMR (100 MHz, CDCl_3) δ 191.1, 169.0, 155.8, 154.5, 137.6, 128.6, 128.4, 127.2, 118.0, 97.3, 70.6, 65.1, 55.7, 52.3, 52.2, 51.5, 46.3, 20.5; IR (thin film) ν_{max} 2955, 2932, 1745, 1692, 1632, 1615, 1244, 1207, 1176, 1162, 1138, 1103, 1009, 971, 734, 702 cm^{-1} ; HRMS calcd for $\text{C}_{20}\text{H}_{22}\text{NO}_5$ 356.1498, found 356.1522 (M + H).

Polycyclic Imine (\pm)-113. To a oven-dried 1-dram vial was added *N*-(4-nitrobenzyl)benzimidoyl chloride (**112**) (40 mg, 0.15 mmol), 3-methoxy-6-methyl-7-phenylbicyclo[3.2.1]oct-3-ene-2,8-dione (**7**) (25 mg, 0.097 mmol), and anhydrous toluene (2 mL) followed by the addition of triethylamine (30.0 μL , 0.215 mmol). The reaction was stirred at rt for 24 h while under argon. The reaction was then evaporated *in vacuo* and purified by flash chromatography (SiO_2 , 40:1 CH_2Cl_2 :MeOH) to afford imine **113** as a pale yellow solid (44%, 21 mg, 0.043 mmol). Mp 210–215 °C dec; ^1H NMR (400 MHz, CDCl_3) δ 8.23 (d, $J = 9.0$ Hz, 2 H), 7.98 (d, $J = 7.0$ Hz, 2 H), 7.85 (d, $J = 9.0$ Hz, 2 H), 7.64–7.48 (m, 3 H), 7.40–7.28 (m, 3 H), 7.22 (d, $J = 7.4$ Hz, 2 H), 3.81 (s, 1 H), 3.52 (dd, $J = 10.6, 5.1$ Hz, 1 H), 3.41 (s, 3 H), 2.70 (dd, $J = 5.1, 2.3$ Hz, 1 H), 2.42 (s, 1 H), 2.33 (ddd, $J = 10.3, 6.9, 2.7$ Hz, 1 H), 1.89 (t, $J = 2.3$ Hz, 1 H), 1.26 (d, $J = 7.0$ Hz, 3 H); ^{13}C NMR (100 MHz, CDCl_3) δ 207.9, 177.0, 147.5, 142.1, 136.8, 132.2, 130.5, 129.8, 129.2, 128.4, 128.2, 127.6, 127.3, 123.4, 103.2, 90.8, 88.4, 61.4, 57.4, 56.2, 56.1, 54.1, 40.9, 20.5; IR (thin film) ν_{max} 2959, 1750, 1603, 1518, 1497, 1448, 1349, 1271, 1151, 910, 853, 732, 697 cm^{-1} ; HRMS calcd for $\text{C}_{30}\text{H}_{27}\text{N}_2\text{O}_5$ 495.1920, found 495.1915 (M + H).

Polycyclic Amine (\pm)-114.



To an oven-dried 1-dram vial was added polycyclic imine **113** (30 mg, 0.061 mmol) followed by the addition of MeOH (1 mL). Next was added NaCNBH_3 (46 mg, 0.73 mmol) and acetic acid (42 μL , 0.73 mmol). The reaction was capped and stirred at rt for 1 h. The reaction was extracted into CH_2Cl_2 (10 mL) and washed with water (2×10 mL) then brine (10 mL). The organic portion was dried over Na_2SO_4 and evaporated *in vacuo*. The resulting residue was purified by flash chromatography (SiO_2 , 20:1 CH_2Cl_2 :MeOH) to afford amine **114** as a pale yellow solid (91%, 28 mg, 0.056 mmol). Mp 225–230 °C dec; ^1H NMR (400 MHz, CDCl_3) δ 8.17 (d, $J = 8.6$ Hz, 2 H), 7.74 (d, $J = 9.0$ Hz, 2 H), 7.56 (d, $J = 7.4$ Hz, 2 H), 7.44 (t, $J = 7.6$ Hz, 1 H), 7.37–7.21 (m, 5 H), 7.14 (d, $J = 7.4$ Hz, 2 H), 5.10 (d, $J = 2.0$ Hz, 1 H), 3.80 (s, 3 H), 3.23 (dd,

$J = 10.7, 5.3$ Hz, 1 H), 2.81 (d, $J = 3.1$ Hz, 1 H), 2.66 (br s, 1 H), 2.39 (dd, $J = 5.1, 2.3$ Hz, 1 H), 2.07–1.94 (m, 1 H), 1.89 (br s, 1 H), 0.95 (d, $J = 7.0$ Hz, 3 H); NOED (400 MHz, CDCl_3) irradi. δ 5.10 (H_a) 3% enhancement at Me_c , 5% enhancement at H_b ; irradi. δ 3.80 (Me_c) 2% enhancement at H_a , 3% enhancement at H_b ; ^{13}C NMR (100 MHz, CDCl_3) δ 210.8, 147.5, 142.1, 139.2, 137.3, 129.0, 128.6, 128.3, 128.2, 127.3, 127.1, 127.0, 123.4, 95.2, 89.3, 79.7, 63.6, 61.0, 53.7, 53.0, 52.3, 50.6, 42.8, 20.3; IR (thin film) ν_{max} 2959, 1744, 1602, 1521, 1496, 1456, 1349, 1152, 1031, 853, 754, 699 cm^{-1} ; HRMS calcd for $\text{C}_{30}\text{H}_{29}\text{N}_2\text{O}_5$ 497.2076, found 497.2063 (M + H).

Acknowledgment. This work was generously supported by Pfizer, Inc., the NIGMS CMLD Initiative (P50 GM067041), and Merck Research Laboratories. We thank

Dr. Emil Lobkovsky (Cornell University) for X-ray crystal structure analyses and Professors John Snyder, James Pánek, Scott Schaus, and Michael Pollastri (Boston University) for helpful discussions. We thank the NSF-REU program (CHE-0649114) for support of Chuan-Xing Ho (Summer, 2007), the Microsystem Technology Laboratories of MIT for help with microreactor fabrication, and Dr. Edward R. Murphy for assistance and advice in establishing the microfluidics screening system.

Supporting Information Available: Complete experimental procedures and compound characterization data including X-ray crystal structure data for **7**, **83**, **89**, **100**, and **113**. This material is available free of charge via the Internet at <http://pubs.acs.org>.